Geoderma 360 (2020) 114037

Contents lists available at ScienceDirect

Geoderma

journal homepage: www.elsevier.com/locate/geoderma

Soil microaggregates store phytoliths in a sandy loam

Zimin Li[a,*], Félix de Tombeur[b], Charles Vander Linden[a], Jean-Thomas Cornelis[b], Bruno Delvaux[a]

[a] Earth and Life Institute, Soil Science, Université catholique de Louvain (UCLouvain), Croix du Sud 2/L7.05.10, 1348 Louvain-La-Neuve, Belgium
[b] TERRA Teaching and Research Centre, Gembloux Agro-Bio Tech, University of Liege, 5030 Gembloux, Belgium

ARTICLE INFO

Handling editor: Yvan Capowiez

Keywords:
Phytolith entrapment
Soil microaggregates
Bioavailable silicon
No-tillage

ABSTRACT

Phytoliths are fine silt-sized amorphous silica particles that form in living plant tissues. Once deposited in soils through plant debris, they may dissolve and increase the fluxes of silicon (Si) towards the biosphere and hydrosphere, thus enhancing positive Si impacts on e.g., plant health and carbon fixation by marine diatoms. Here we analyzed the role of soil aggregates in phytolith protection against dissolution. We investigated the distribution of phytoliths in the size fractions of a sandy loam topsoil subjected to two long-term treatments: conventional (CT) and no tillage (NT). The topsoil size fractions were separated through wet sieving and named, respectively: macroaggregates (250–2000 μm), free microaggregates (50–250 μm), and silt + clay (< 50 μm). Protected microaggregates held within macroaggregates were extracted using a constant and continuous water flow process. We assessed the pool of phytoliths through heavy liquid separation and alkaline dissolution (Na_2CO_3), and we assessed the bioavailability of Si using $CaCl_2$ extraction. As expected, NT generates larger amounts of aggregates than CT. Concentrations and stocks of phytoliths determined by heavy liquid separation are ten times higher than those measured by Na_2CO_3 in bulk soil and size fractions. Soil microaggregates contribute for over 60% to the pool of phytoliths, which control bioavailable Si. The release of bioavailable Si from microaggregates is slower than that from the silt + clay fraction, suggesting that soil microaggregates can trap phytoliths and protect them from rapid dissolution. No-tillage and associated conservation agricultural practices may thus promote the stabilization of phytoliths in soils and decrease their dissolution rate. We propose that the entrapment of phytoliths in soil aggregates may be one of the processes favoring the persistence of phytoliths in soils and sediments. We expect that this persistence should be enhanced in strongly aggregated soils.

1. Introduction

Plants take up silicon (Si) as aqueous $H_4SiO_4^0$ from soil solution, and form phytogenic silica (PhSi) bodies. These silicified structures encompass phytoliths and fragile, small-scaled silica particles (< 5 μm) that return to soil with plant debris (Smithson, 1956; Puppe et al., 2017). Phytoliths dissolve at common pH values (4.5–8) of soil solution (Fraysse et al., 2006) whereby small-scaled phytoliths (< 5μm) are water-soluble (Puppe et al., 2017). The dissolution rate of phytoliths is one to two orders of magnitude higher than that of typical soil clay and parent-rock primary silicate minerals (Fraysse et al., 2009). By releasing plant available Si, PhSi particles may provide plant disease regulation and tolerance to abiotic stresses (Coskun et al., 2019). Besides, their formation originally derives from silicate weathering, which consumes carbon dioxide (Berner, 1997). The soil-to-plant Si cycle thus tremendously influences the global Si cycle (Conley, 2002). It is therefore crucial to identify the factors impacting the dissolution of PhSi bodies and the subsequent release of dissolved Si (DSi), which contributes to the stock of bioavailable Si in soil.

Under given environmental conditions, the dissolution of phytoliths depends on plant species and phytolith composition, water content, and surface properties (Bartoli and Wilding, 1980; Fraysse et al., 2006; Li et al., 2014; Puppe and Leue, 2018) whereas the amount of phytoliths accumulating in soil depends on soil weathering stage (Cornelis and Delvaux, 2016) and soil properties/processes such as soil acidity and Al loading (Bartoli, 1985; Bartoli and Wilding, 1980). For a given pool of phytoliths as estimated by the *DeMaster* technique (DeMaster, 1981), the release of bioavailable Si, as assessed by $CaCl_2$ (Cornelis et al., 2011) or NH_4OAc extraction (Saccone et al., 2007), differs according to soil type as illustrated in Fig. 1. This graph illustrates the impact of soil–plant interactions on bioavailable Si (as assessed by $CaCl_2$ and NH_4OAc extractions), notably the well-known role of grasses on the magnitude of the phytolith pool and its reactivity in Chernozems (Blecker et al., 2006; White et al., 2012). Furthermore, it suggests that the control of phytoliths in soils on bioavailable Si depends on the soil–plant system. Soil type indeed affects Si bioavailability through soil

* Corresponding author.
E-mail address: zimin.li@uclouvain.be (Z. Li).

https://doi.org/10.1016/j.geoderma.2019.114037
Received 24 June 2019; Received in revised form 21 October 2019; Accepted 23 October 2019
Available online 23 November 2019

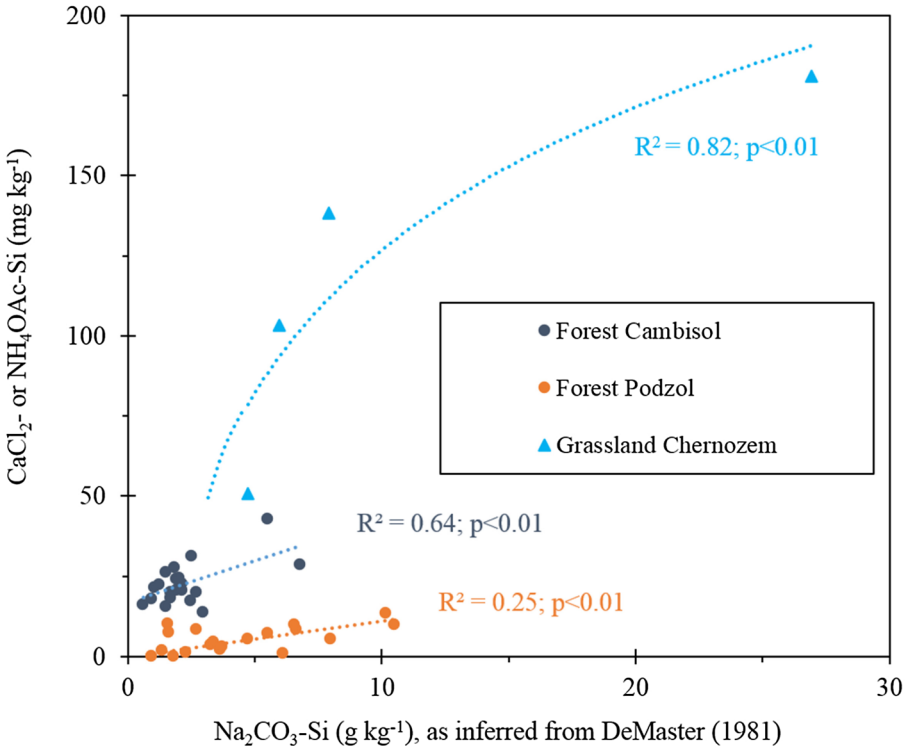

Fig. 1. Plot of plant available Si content (assessed by $CaCl_2$ 0.01 M or NH_4OAc 0.5 M) against phytolithic Si content (assessed by Na_2CO_3 after DeMaster, 1981) in surface soils (00–20 cm) in different soil–plant systems. Podzols (New Hampshire, USA; pH_{CaCl2} = 3.9–4.6) under forest sugar maple *Acer saccharum*, yellow birch *Betula alleghaniensis,* and beech *Fagus grandifolia* (Saccone et al., 2007). Cambisols (Morvan, France; pH_{CaCl2} = 3.8–4.8) under Douglas fir (*Pseudotsuga menziesii*), Black pine (*Pinus nigra*) and European beech (*Fagus sylvatica* L.) (Cornelis et al., 2011). Chernozems (Northeastern/Central Colorado and Kansas, USA; pH_{CaCl2} = 5.2–5.9) under grasslands: 2 sites under short-grasses dominated by *Bouteluoa gracillis* and *Buchloe dactyloides*, 1 site under mixed grasses *Festuca* sp. and *Bouteluoa gracillis*, 1 site under tall grasses site dominated by *Antropogon gerardi*. Plant available Si was extracted by $CaCl_2$ 0.01 M in the Cambisol, but by NH_4OAc 0.5 M in the Podzol and Chernozem (Saccone et al., 2007). (For interpretation of the references to colour in this figure legend, the reader is referred to the web version of this article.)

weathering stage (Cornelis and Delvaux, 2016; Henriet et al., 2008; Klotzbücher et al., 2015; Melzer et al., 2012); Al loading of phytolith surface (Bartoli, 1985; Bartoli and Wilding, 1980), pH (Fraysse et al., 2009; Meunier et al., 2018) and soil buffering capacity (Li et al., 2019), which in turn depends on soil composition and surface properties (Li et al., 2019). Fig. 1 may also suggest that the release of plant available Si might be affected by soil aggregation. Indeed, the soil diversity in Fig. 1 may represent a gradient in soil aggregation from the structureless Podzol to the highly aggregated Chernozem. Our hypothesis is that phytoliths may be stored in soil aggregates and that their protection impacts their dissolution and dissolution rate. Following that assumption, soil processes that promote soil aggregation, i.e. the transformation of soil organic matter (SOM) and mineral weathering, would thus contribute to store PhSi bodies, increase the pool of phytoliths, and thus plant available Si originating from phytolith dissolution if these silica bodies are protected.

An ample literature is available on the storage of organic C (OC) in soil aggregates (< 250 µm) (Baldock and Skjemstad, 2000; Balesdent et al., 2000; Chenu et al., 2019; Kleber et al., 2015; Lal, 2004; Oades, 1984; Paustian et al., 1997; Six et al., 2002, 1999, 1998, 2000a, 2004; Stockmann et al., 2013; Totsche et al., 2018; Wiesmeier et al., 2019). In particular, microaggregates protect SOM in the long term, and macroaggregate (> 250 µm) turnover is a crucial process to stabilize SOM (Six et al., 2004). Soil tillage may enhance decomposition of OC by exposing SOM physically protected in microaggregates (Balesdent et al., 2000). In this respect, conventional tillage (CT) and no-tillage (NT) practices differently impact the aggregate dynamics in the topsoil: a faster turnover of macroaggregates in CT compared with NT leads to a slower rate of microaggregate formation within macroaggregates and less stabilization of SOM under CT (Six et al., 1999; 2000a). Totsche et al. (2018) have highlighted that little is known concerning the role microaggregates play in the fate of elements like Si, Fe, Al, P, and S. Given the fine silt-size and relatively high surface area of phytoliths (Bartoli, 1985; Bartoli and Wilding, 1980; Fraysse et al., 2006, 2009), it is likely that they might be entrapped in soil microaggregates. Here we investigate the distribution of phytoliths as a function of aggregate size in a sandy loam subjected to long term CT and NT practices. We study this distribution in the bulk soil and size fractions separated through wet sieving according to different size classes. We further quantify phytoliths through physical extraction and Na_2CO_3 dissolution, and we assess bioavailable Si using $CaCl_2$ extraction.

2. Materials and methods

2.1. Study site and soil sampling

The experimental site is located at Wiers, Demasy Farm (N 50° 2́956″, E 3° 3́015″), Western Belgium (Fig. S1), under a temperate climate. The mean annual precipitation and temperature are 800 mm and 10 °C, respectively. The experimental field includes three replicates of paired-sites under long-term conventional tillage (CT) and no tillage (NT) practices (CT1-3, NT1-3, Fig. S1). Previously, the entire area was cultivated in conventional mode (CT). From 1995 onwards, parts of the area were cultivated without tillage and practicing direct seeding (NT). The cultivated soil under CT is used for a wheat – maize rotation with regular exportation of total crop straws (Table S1). The pasture soil under NT is used for wheat –maize – barley/grass/legumes – cover crop rotation, which is practiced while retaining stubbles in the field, returning straws after harvesting, and performing direct seeding (Table S1). The soil has a sandy loam texture, and is classified as a Retisol (IUSS, 2014).

Soil samples were collected one week before crop harvesting in July 2015, i.e., 20 years after the beginning of the experiment. For each individual plot (CT1-3, NT1-3), a composite bulk soil of 6 undisturbed cores was built up from the topsoil (0–20 cm) in a random triangle distribution (3 m distance between two soil sampling sites). Additional core samples were collected to determine bulk density and soil moisture content (n = 3). Table 1 gives an overview of the replications.

2.2. Separation of size fractions

The soil samples were air-dried at room temperature, gently broken by hand along weakness planes, and sieved at 8 mm. We removed 'aggregate-free' organic debris, plant roots (> 2 mm), visible fauna and

Table 1
Overview of the replications and deduction of the number of replicates used for statistical analyses.

Treatment	CT			NT			n =
3 plots	CT1	CT2	CT3	NT1	NT2	NT3	9
Bulk soil samples	3	3	3	3	3	3	9
Undisturbed soil samples (bulk density)	3	3	3	3	3	3	9
Basic properties (pH, CEC, C, N…)	3	3	3	3	3	3	9
Elemental analysis	3	3	3	3	3	3	9
Particle size analysis	1	1	1	1	1	1	3
XRD	1	1	1	1	1	1	3
SEM	1	1	1	1	1	1	3
Size fractions (< 50, 50–250, 250–2000 μm)	3	3	3	3	3	3	9
$CaCl_2$-Si	3	3	3	3	3	3	9
Na_2CO_3-Si	3	3	3	3	3	3	9
*hl*PhSi	3	3	3	3	3	3	9

gravels and sieved the samples at 2 mm. The separation of size fractions was done by wet sieving of the bulk soil (< 2 mm) using the procedure of Six et al. (1998). The size fractions include isolated particles as well as soil aggregates. However, following Six et al. (1998), we used the terms "macroaggregates", "microaggregates" and "silt + clay" in our article to facilitate readability. An 80 g subsample was submerged under deionized water on a 250 μm sieve for 5 min at room temperature. Subsequently, 50 repetitions of a top-down movement for 2 min (by immersing and emerging the net of the sieve in deionized water) allowed the separation of the coarse fractions (> 250 μm), designated as macroaggregates. Water and soil materials < 250 μm were quantitatively transferred for the second wet sieving at 50 μm. The process was repeated to collect the free microaggregates (50–250 μm) and silt + clay fractions (0–50 μm). Extracting protected microaggregates held within macroaggregates was carried out with 10 g of macroaggregates placed on top of a 250 μm screen and shaken with 50 glass beads (4 mm in diameter, 10–15 min) (De Tombeur et al., 2018) under a constant and continuous water flow using the device and procedure established by Six et al. (2000b). Macroaggregates, free microaggregates, protected microaggregates, and silt + clay fractions were oven-dried at 60 °C (n = 9, Table 1).

2.3. Physico-chemical analyses of bulk soils and size fractions

Exchangeable cations (K, Ca, Na and Mg) and cation exchange capacity (CEC) were determined (n = 9) according to Chapman (1965) using 1 M ammonium acetate buffered at pH 7; pH was measured in H_2O and 1 M KCl using 5 g:25 mL suspensions. Soil texture was determined in triplicate (n = 3) using a Beckman Coulter device (LSTM-133320) to quantify the particle size distribution of sand (2 mm–50 μm), silt (50 – 2 μm) and clay (< 2μm). Total elemental concentrations (K, Ca, Na, Mg, Si, Al and Fe) were measured (n = 9) by inductively coupled plasma/atomic emission spectrometry (ICP–AES, Jarrell Ash Iris Advantage) after alkaline fusion using Li-metaborate + Li-tetraborate at 1000 °C, followed by ash dissolution with 10% HNO_3 (Chao and Sanzolone, 1992). The concentrations of major alkaline and alkaline-earth cations (K, Ca, Na and Mg; n = 9) were summed up to compute the Total Reserve in Bases (TRB) (Herbillon, 1986). Total C and N concentrations were measured using a Flash 2000 Elemental Analyzer (Thermo Fisher Scientific, Waltham, MA, USA). Crystalline minerals were identified through powder X-ray diffraction (XRD) (n = 3) using Cu-Kα radiation in a Bruker Advance diffractometer. Scanning Electron Microscopy coupled with Energy Dispersive X-ray analysis (SEM-EDX) was carried out without any chemical pretreatment using a field emission gun SEM (FEG-SEM; Zeiss Ultra55) (n = 9).

2.4. $CaCl_2$ and Na_2CO_3 extractions of Si, physical extraction of soil phytoliths in bulk soils and size fractions

2.4.1. $CaCl_2$-extractable Si content

($CaCl_2$-Si) is considered to assess bioavailable Si in soils (Haysom and Chapman, 1975; Sauer et al., 2006). We measured it through a kinetic extraction (Li et al., 2019) using a solid:liquid ratio 5 g:50 mL (0.01 M $CaCl_2$) in 100 mL polyethylene cups shaken at 25 °C (n = 9). The 1:10 solid:liquid ratio was kept constant using replicates for both the extraction and analysis. At each time step (6, 12, 24 h; 2, 4, 8, 16, 32 and 64 days), the collected suspension (50 mL) was centrifuged at 3,000g for 20 min. The supernatant (40 mL) was filtered and separated in two aliquots of 20 mL to measure pH and solutes concentrations, respectively. The latter extract was acidified by adding 100 μl of HNO_3 7 M to analyze Si concentration by ICP-AES.

2.4.2. Na_2CO_3 extractable Si content

(Na_2CO_3-Si) is routinely measured to assess biogenic silica in soils and sediments (DeMaster, 1981; Koning et al., 2002; Saccone et al., 2006). It is used here to evaluate chemically the pool of PhSi bodies, expressed as elemental Na_2CO_3 extractable Si content (Na_2CO_3-Si) (n = 9), assuming that other forms of biogenic silica (Puppe et al., 2015) would occur in minor amounts. Thirty mg of bulk soil or aggregate fraction was mixed in 40 mL of 0.1 M Na_2CO_3, pH = 11.2, and digested for 5 h at 85 °C. One ml of extraction solution was taken at 1, 2, 3, 4 and 5 h, then acidified by adding 100 μl of HNO_3 7 M to analyze dissolved Si using ICP-AES. The extracted Si (mg g^{-1}) was plotted against time (DeMaster, 1981). We corrected for the simultaneous alkaline dissolution of amorphous and crystalline Si using time course extraction (DeMaster, 1981; Koning et al., 2002), assuming that (a) most of the amorphous pool is dissolved within the first 2 h of extraction (DeMaster, 1981), and (b) the clay minerals release Si at a much slower and constant rate during the whole extraction. The Na_2CO_3-Si concentration was determined by the intercept of the linear part of the plot, using the lm function of the R programming language to fit a first-order kinetic model (Cornelis et al., 2011).

2.4.3. Physical extraction of soil phytoliths

*hl*PhSi refers to the elemental content of phytogenic Si from phytoliths physically extracted using heavy liquid (*hl*) separations (Kelly, 1990). Five g of bulk soil or size fraction were treated by H_2O_2 (6%) at 70 °C for three days until complete oxidation of SOM (n = 9). HCl (15%) was then added to remove free iron oxides and carbonates if present. The $H_2O_2^-$ and HCl-treated sub-samples were submitted to an additional overnight dispersion with Na^+-saturated resins to eliminate any clay contamination (Rouiller et al., 1972). The sub-samples were mixed with 40 mL of sodium polytungstate (Na_6 ($H_2W_{12}O_{40}$) H_2O, density = 2.35 g cm^{-3}) to separate phytoliths, and centrifuged at 4000 rpm for 20 mins. After centrifugation, the supernatant including the floating phytoliths was removed with a pipette, and collected in a glass vessel through a Teflon filter at 2 μm (polytetrafluoroethylene: PTFE) soaked with methanol. The filter was then abundantly rinsed with HCl 1 M and then washed with deionized water. The subsample was then remixed with 40 mL of sodium polytungstate (2.35 g cm^{-3}) and again centrifuged at 4000 rpm for 20 mins. The operation was repeated until the supernatant was clear. The filter was dried at 105 °C for gravimetrical quantification. XRD was carried out on extracted materials to check the purity of the phytoliths while SEM analyses were performed on extracted phytoliths to observe their morphology. To compare with the 1% Na_2CO_3 method, we calculated the Si content from the total sample weight (Meunier et al., 2014). Assuming a phytolith mean water content of 10% (equivalent to 0.37 mol of H_2O per 2 mol of SiO_2), 42% of the measured weight of phytoliths would be Si (Alexandre et al., 1997). This content of Si thus deduced is referred to as *hl*PhSi.

2.5. Data analyses

Arithmetic means, standard deviations of all measured variables, and statistical tests were performed using SPSS 24.0 software. The significance of the difference between measured arithmetic means in CT and NT was measured with the independent-Sample T separation test at the $p < 0.05$ level. When arithmetic means significantly differ between CT and NT, they are presented with a different lowercase letter. The significance of the difference between measured arithmetic means for the macroaggregates, free microaggregates, protected microaggregates, and silt + clay fractions was tested using a Tukey's mean separation test at the $p < 0.05$ level. Significantly different arithmetic means are presented with different lowercase letters.

The stocks of C, N, $CaCl_2$-Si, Na_2CO_3-Si and *hl*PhSi in bulk soil and size fractions were calculated according to Eqs. (1) and (2), respectively, as described in Supplementary Information.

3. Results

3.1. Soil properties and aggregate distribution

Texture, mineral constitution, CEC, pH and base saturation did not statistically differ between CT and NT, while C and N contents differed (Figs. S2 and S3; Tables S2–S3). The larger C and N contents in NT than in CT directly resulted from the NT practices as reported in previous studies (Abiven et al., 2009; Blanco-Canqui and Lal, 2008; Bronick and Lal, 2005; Oades, 1984; Poeplau and Don, 2015; Six et al., 2000a,b; Six et al., 2004; West and Post, 2002). The mass distribution of soil size fractions (designated as aggregates) differed between CT and NT, but was dependent on the aggregate size (Fig. 2). The contribution of macroaggregates and protected microaggregates to bulk soil did not differ. In contrast, silt + clay decreased whereas free microaggregates increased in NT relatively to CT (Fig. 2). Free microaggregates contributed to 61% of bulk soils in NT against 54% in CT. SEM analyses (Fig. 3) revealed the occurrence of phytoliths in the bulk soils and size fractions.

3.2. Chemical and physical extractions of Si in bulk soils and size fractions (aggregates)

The experimental data are presented in terms of Si concentration (g kg^{-1}) and stock (g m^{-2}) in Figs. 4, 5.

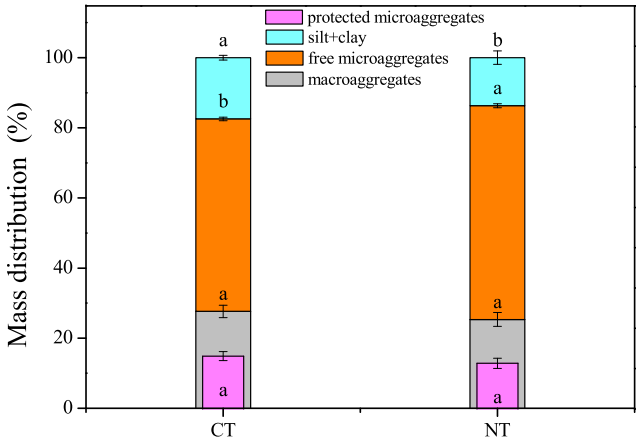

Fig. 2. Mass distribution between conventional tillage (CT) and no tillage (NT) of macroaggregates (250–2000 μm), free microaggregates (50–250 μm), protected microaggregates (50–250 μm), silt + clay (< 50 μm) in three plots. The average values shown with different lowercase letters (a, b) between CT and NT significantly differ at the $p < 0.05$ level of confidence according to independent-Samples T – separation test (n = 9).

3.2.1. *hl*PhSi content and stock

In bulk soil, *hl*PhSi was significantly larger in NT than in CT (Fig. 4): the content (g kg^{-1}) was 9 in NT and 7 in CT whereas the stock (g m^{-2}) was 2667 in NT and 1923 in CT. In the aggregate fractions, *hl*PhSi content was invariably larger in NT than in CT (Fig. 4a); the same trend is observed for the *hl*PhSi stock, except in protected microaggregates and silt + clay at least at $p < 0.05$. Furthermore, whatever the treatment (CT or NT), *hl*PhSi content and stock in aggregate fractions were the largest in free microaggregates, and the lowest in macroaggregates (Fig. 4a–b). The *hl*PhSi content (g kg^{-1}) in free microaggregates was 6.8 in NT and 5.1 in CT, whereas the *hl*PhSi stock (g m^{-2}) in free microaggregates was 1208 in NT and 762 in CT.

3.2.2. Na_2CO_3-Si content and stock

The Na_2CO_3-Si content was assessed from the kinetic dissolution curves (Fig. S4). Unlike *hl*PhSi content, Na_2CO_3-Si content and stock in bulk soil did not differ between NT and CT (Fig. 4c-d). In the aggregate fractions, Na_2CO_3-Si content (g kg^{-1}) in macroaggregates was larger in CT (0.43) than in NT (0.30) (Fig. 4c–d). Whatever the treatment (CT or NT), the Na_2CO_3-Si content and stock were the largest in the silt and clay fraction, and the lowest in macroaggregates (Fig. 4c–d). Considering both the bulk soil and the aggregate fractions, it is interesting to note that the concentration ratio [*hl*PhSi/Na_2CO_3-Si] in CT was 1.2 in silt + clay, and ranged from 5.7 to 7.8 in bulk and aggregate fractions (Table 2). As compared to that respective value in CT, this ratio was significantly higher ($p < 0.01$) in NT: 2.2 in silt + clay, from 7.8 to 11.3 in bulk and aggregate fractions (Table 2). Besides, for both CT and NT treatments, this ratio was significantly ($p < 0.01$) higher in bulk soil, macroaggregates and microaggregates (5.7–11.3) than in silt + clay (1.2–2.2).

3.2.3. $CaCl_2$-Si content and stock

$CaCl_2$-Si content and stock in bulk soil were larger in NT than in CT (Fig. 4e–f), but only significantly for the stock. The content (mg kg^{-1}) was 225 in NT and 207 in CT, whereas the stock (g m^{-2}) was 66 in NT and 57 in CT (Fig. 4e–f). In aggregate fractions, $CaCl_2$-Si content was significantly larger in NT than in CT (Fig. 4e–f) except in macroaggregates ($p = 0.088$) whereas $CaCl_2$-Si stock significantly differed between CT and NT in free microaggregates. Whatever the treatment, $CaCl_2$-Si content was the largest in protected and free microaggregates, (Fig. 4e–f), but the lowest in silt + clay. The $CaCl_2$-Si content represents at most 5.9% of the phytolithic Si concentration (*hl*PhSi) (Fig. 4). This percentage was invariably higher in CT than in NT. Indeed it is, respectively, in CT and NT (%): 3.3 and 2.7 in bulk soil, 5.5 and 5.9 in macroaggregates, 2.6 and 2.3 in free microaggregates, 4.6 and 4.5 in protected microaggregates, 2.7 and 2.4 in silt + clay. As inferred from Fig. 5, $CaCl_2$-Si content (mg kg^{-1}) at day 64 was in the range 207–225 in bulk soil, 133–198 in macroaggregates, free microaggregates and protected microaggregates, 97–125 in silt + clay, whatever the treatment. The extraction rate rapidly decreased in silt + clay. In contrast, the extraction kinetics did not reach a plateau in bulk soil and, to a lesser extent, in the aggregates, particularly in free microaggregates. In both CT and NT, the concentration of H_4SiO_4 in the $CaCl_2$ extract increased from $\sim 10^{-4.6}$ to $\sim 10^{-3.4}$ – $10^{-3.1}$ mol l^{-1} with increasing extraction time (6 h to 64d), as reported in Table S4, whereas pH ranged between 5.96 and 4.94. This table also showed that the concentration of Al was extremely low ($10^{-6.8}$–$10^{-4.8}$ mol l^{-1}). The data presented in Table S4 were used to illustrate the influence of pH on aqueous H_4SiO_4 concentration and identify the solid phases that control this concentration (see Discussion).

3.3. Morphological features of phytoliths in bulk soils and aggregates

As illustrated in Fig. 6, phytolith particles were observed in all soil fractions, whatever the tillage practices. A careful examination of the micrographs showed that phytolith particles were silt-sized, notably

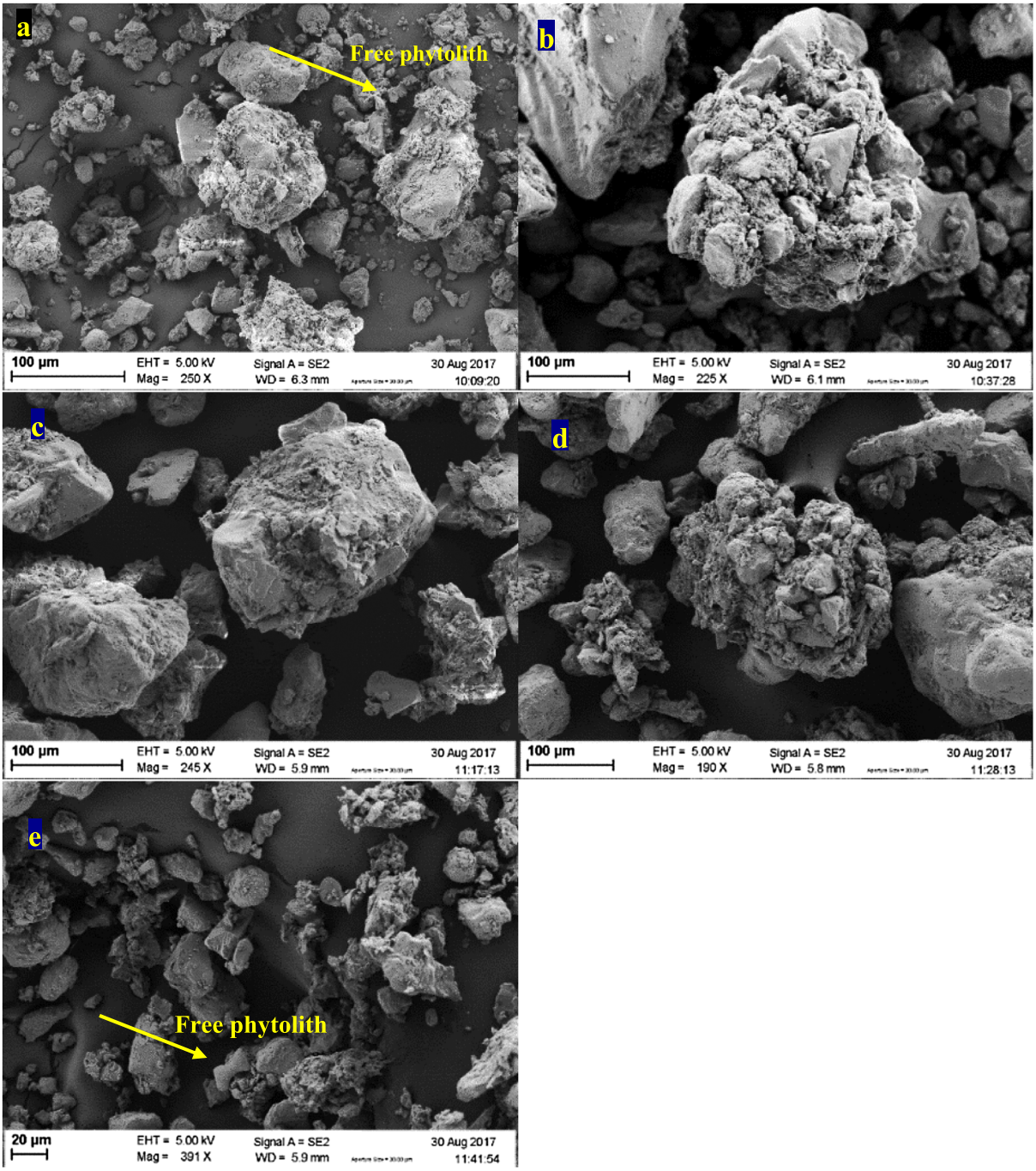

Fig. 3. SEM micrographs performed on: (a) bulk soil, (b) macroaggregates, (c) free microaggregates, (d) protected microaggregates, (e) silt + clay. The sub-samples of bulk soil and aggregates were from plot 2 in CT.

fine silt-sized (< 20 µm). Besides, the inspection of their surface morphological features revealed a much higher density of dissolution cavities in the silt + clay fraction. As shown in Fig. 6, this density amounted to 15 and 41 dissolution cavities per 100 μm^2 in NT and CT respectively against 5 in macroaggregates, 2 in free microaggregates, 2 and 4 in protected microaggregates. These dissolution cavities were similar to the ones previously detected from dissolution experiments (see Fig. 4.F-G in Fraysse et al., 2009). Most likely, the dissolution features observed in silt + clay could be attributed to a larger exposure of silt-sized phytolith particles to dissolution in this size fraction in both CT and NT.

4. Discussion

The discussion of our results aims at challenging three questions. (**1**) What is the solid phase that controls bioavailable Si ($CaCl_2$-Si)? (**2**) Do the cultural practices affect the phytolith pool and Si bioavailability? (**3**) Do soil aggregates protect phytoliths against rapid dissolution? Finally, we question the *DeMaster* technique (DeMaster, 1981) to quantify phytoliths in soils.

4.1. Control of Si bioavailability in soil by phytoliths

Analytical data from Table S4 show a time-dependent increase in the concentration of H_4SiO_4 as previously observed (Li et al. 2019).

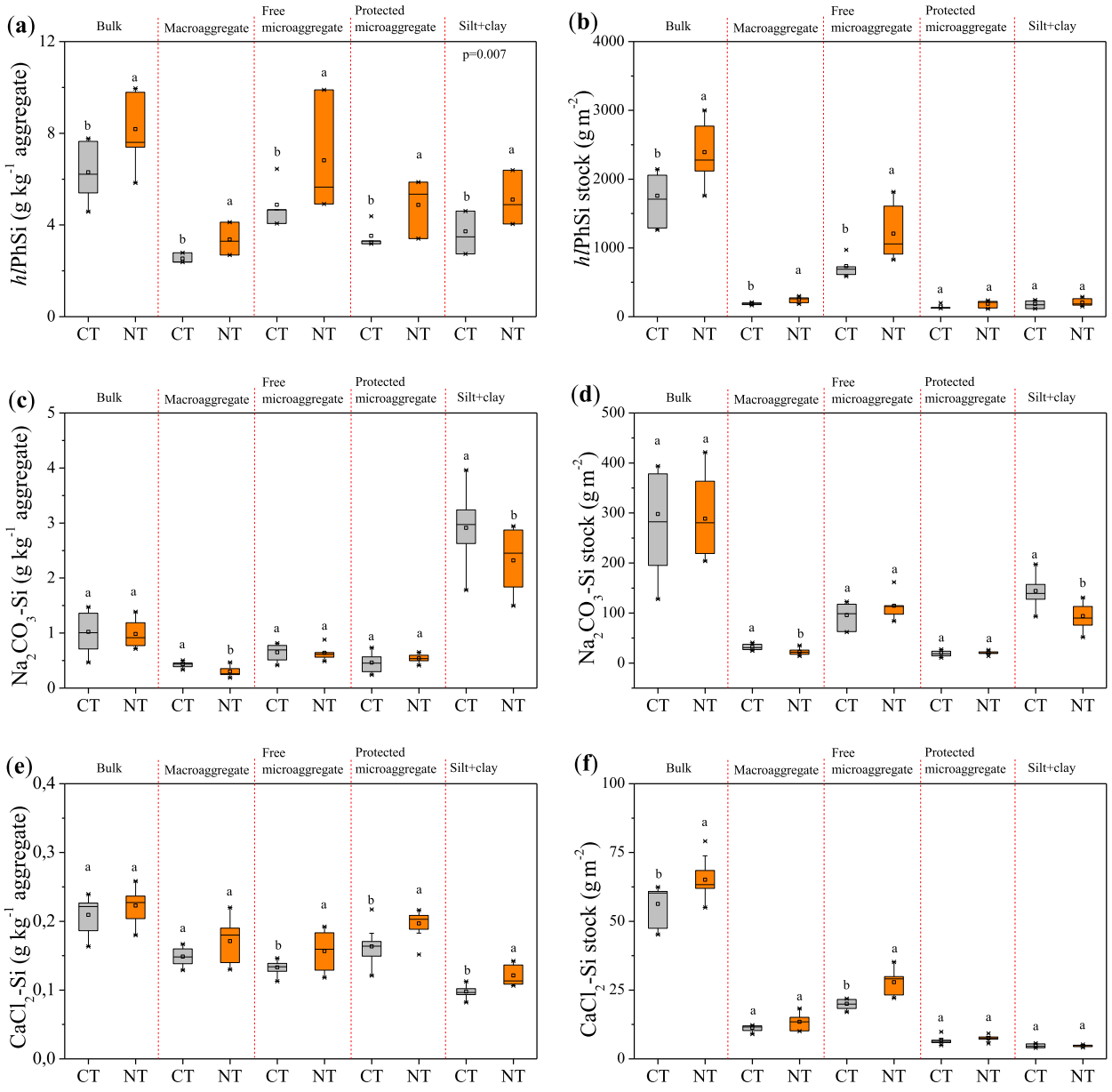

Fig. 4. Box plot of Si concentration (left) and stock (right) in bulk soil and aggregates in CT and NT. (a–b): *hl*PhSi (heavy liquid separation), (c-d): Na_2CO_3-Si, (e–f): $CaCl_2$-Si. Different lowercase letters (a, b) are significantly different according to independent T-test between CT and NT ($n = 9$, $p < 0.05$) over all crop plots. $CaCl_2$-Si is the cumulative amount of Si at the 64th day of the kinetic extraction. Note: square denotes the average values; star denotes the maximum and minimum value, respectively; cross denotes an error line through a maximum and minimum value, respectively.

That concentration at the 64d extraction time decreases with increasing pH_{CaCl2} from 4.9 to 5.7 (Figure S5a). Figure S5b suggests that H_4SiO_4 concentration might be controlled by smectite clay minerals, which occur in the clay fraction (Figure S2a), and by amorphous silica, but not by quartz (Karathanasis, 2002; Lindsay, 1979). In the beidellite-montmorillonite series of smectite clay minerals, the Si:Al atomic ratio theoretically ranges between 2.85 and 1.5, while it is 1.0 in kaolinite. Given the extremely low Al concentrations in $CaCl_2$ extracts, we can exclude a control of $CaCl_2$-Si concentration by clay minerals, and propose that PhSi bodies control the concentration of H_4SiO_4 concentrations in $CaCl_2$ extracts (Figure S5c).

4.2. *Effects of tillage practices on phytolith pool and Si bioavailability in soil*

Previous studies suggest that conventional, intensive agricultural practices decrease the pool of bioavailable Si in soils because of crop harvest and removal of crop straws (Carey and Fulweiler, 2016; Clymans et al., 2011; Guntzer et al., 2012; Haynes, 2017; Keller et al., 2012; Struyf et al., 2010; Vandevenne et al., 2012). Our experimental data corroborate these studies since CT encompasses the removal of crop biomass out of cultivated fields whereas NT involves the recycling of inedible crop biomass *in situ*. Indeed, the phytolith pool, as physically extracted by heavy liquid separation, is significantly larger in NT than in CT, resulting from the constant return of crop residues in NT (Fig. 4a-b). The greater pool of $CaCl_2$-Si and *hl*PhSi in NT is thus linked to the recycling of crop biomass similarly to the increase of SOM content following such recycling, no tillage and direct seedling practices (Figure S3). For instance, the larger C and N contents under NT than under CT are direct consequences of tillage practices as already observed in several studies (Blanco-Canqui and Lal, 2008; Six et al., 1999; Six et al., 2000a; West and Post, 2002). The substantial difference in C and N contents and stocks between CT and NT may be ascribed to the following practices under NT: i) cover crops (Bronick and Lal, 2005; Poeplau and Don, 2015), ii) plant straw/residue return (Blanco-Canqui

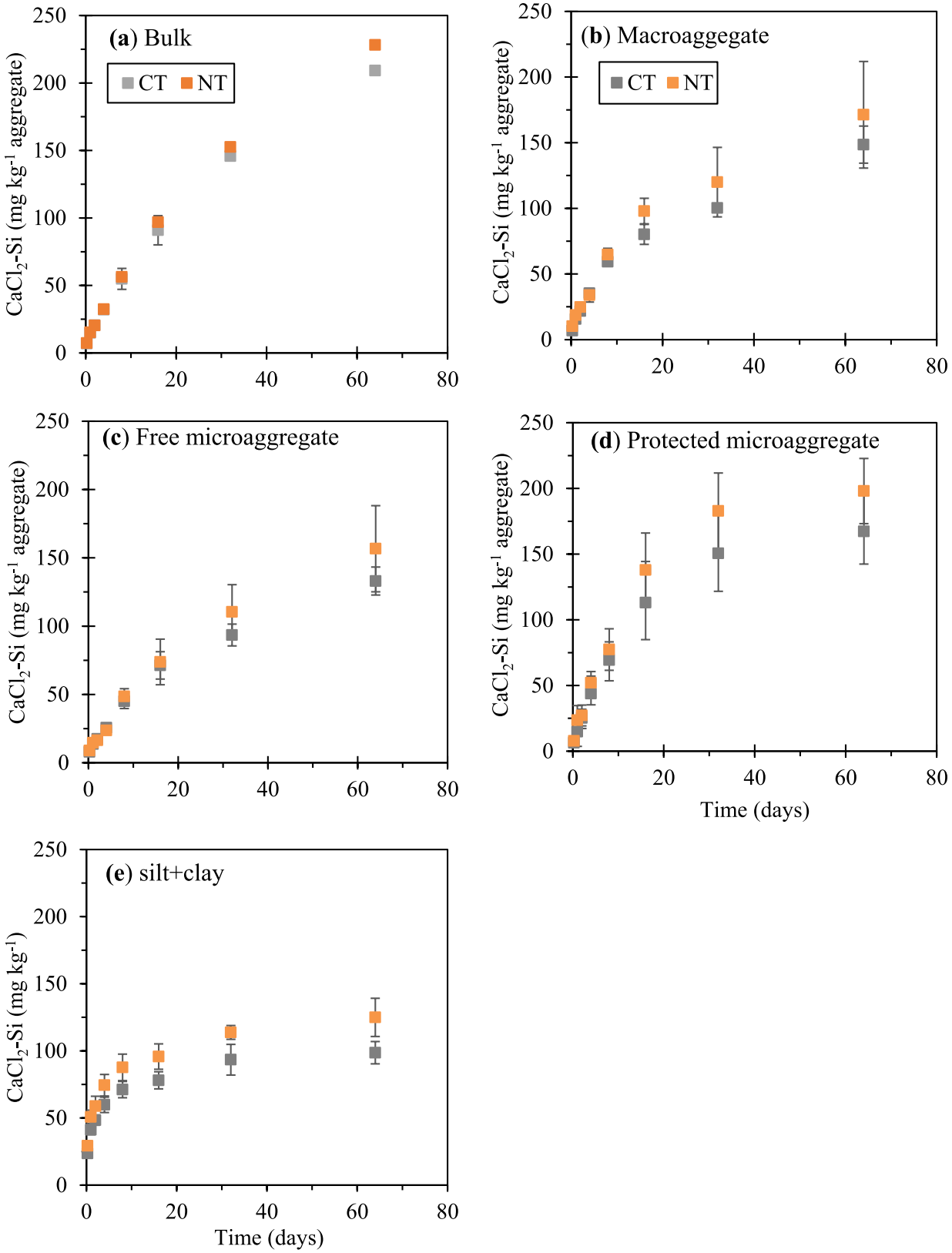

Fig. 5. $CaCl_2$ extractable Si ($CaCl_2$-Si) plotted against time (6 h, 12 h, 24 h, 2, 4, 8, 16, 32, and 64 days. a: bulk soil; b: macroaggregates; c: free microaggregates; d. protected microaggregate; e. silt + clay. CT: conventional tillage; NT: no-tillage (n = 9).

and Lal, 2008; West and Post, 2002) iii) direct seeding (Abiven et al., 2009; Oades, 1984; Six et al., 2004; Six et al., 2000b). In addition, the difference in the reservoirs of bioavailable Si and phytogenic Si between NT and CT is large, despite the cropping of high Si-accumulators in CT with the rotation wheat-maize *versus* maize-wheat-barley/grass/legumes–cover crop in NT, in most experimental field plots (Table S1). Oats and barley have a relatively small Si uptake rate (kg Si ha^{-1}), i.e., 15–30 compared to 30–100 in wheat and 100–130 in maize (Keller

Table 2
The ratio of concentration [*hl*PhSi/Na_2CO_3-Si] in bulk, macroaggregates (250–2000 μm), free microaggregate (50–250 μm), protected microaggregates (50–250 μm), silt + clay (< 50 μm) in CT and NT. The average values with different lowercase letters (a, b) significantly differed at the $p < 0.01$ level of confidence according to independent T-test between CT and NT (n = 9) over all crop plots.

Aggregate size fraction	CT	NT
Ratio of concentration [*hl*PhSi/Na_2CO_3-Si]		
Bulk	5.7b	7.8a
Macroaggregates	5.9b	11.2a
Free microaggregate	7.8b	10.7a
Protected microaggregate	7.5b	9.0a
Silt + clay	1.2b	2.2a

et al., 2012). In natural ecosystems (e.g. unmanaged forests or grasslands), phytoliths return to soil with organic debris, and recycle Si through plant root uptake (Alexandre et al., 1997; Bartoli, 1983; Cornelis et al., 2010; Gérard et al., 2008; Lucas et al., 1993). In contrast, crop harvest and regular Si-rich straw removal (e.g. wheat, maize, rice…) commonly occur in agroecosystems in CT, and lead to the exportation of plant phytoliths (Guntzer et al., 2012; Vandevenne et al., 2012), decreasing the pool of soil PhSi bodies and thus the source of bioavailable Si in soil. Not surprisingly, crop harvest and straw removal at global scale lead to the exportation of 210–224 million tons PhSi yr^{-1} from agricultural soils (Matichenkov and Bocharnikova, 2001), creating a new agricultural Si loop (Vandevenne et al., 2015; Vandevenne et al., 2012). Here, after 20 yrs, the soil phytolith stock (T PhSi per ha) significantly differs between NT (57.08) and CT (44.14) due to the systematic export of crop residues in CT. The initial stock of phytoliths is unfortunately unknown. It is probably between 44 and 58 T PhSi per ha. Assuming an initial stock of 50 T PhSi per ha, the decrease in the stock of phytoliths under CT could be explained by the systematic annual export of crop residues (Guntzer et al., 2012; Struyf et al., 2010; Vandevenne et al., 2015). On the other hand, the increase in this stock is due to the systematic return of crop residues to soil in NT. In any case, the significant difference between CT and NT systems is due to this difference in practices. The increase rate of phytolith stock (7.08 T PhSi per ha within 20 years) in NT would amount to 350 kg ha^{-1} yr^{-1}, much above 35 kg PhSi ha^{-1} yr^{-1} in temperate rice croplands (Desplanques et al., 2006) or 22–67 kg PhSi ha^{-1} yr^{-1} in continental grasslands (Blecker et al., 2006). However, it is comparable to 300 kg Si ha^{-1} yr^{-1} in sugarcane (Meyer and Keeping, 2001), but below 500 kg Si ha^{-1} yr^{-1} in tropical rice cropland (Makabe et al., 2009). Most probably, our overestimation results from practices or processes that may dilute soil phytoliths in CT topsoil, notably by e.g., ploughing (Keller et al., 2012), and breaking down of aggregates in CT (Six et al., 2002; Six et al., 2004).

4.3. Soil microaggregates store and protect phytoliths

As discussed above, the pools of phytoliths and bioavailable Si in soil are larger in NT than in CT because of the return of inedible crop biomass to soil in NT. However, the phytolith pool is much larger in free microaggregates (Fig. 4a) while the pool of bioavailable Si is larger in free and protected microaggregates (Fig. 4e) than in other aggregate fractions. This suggests that NT practices also affect the pools of phytoliths and bioavailable Si in soil through the process of microaggregation. This process is indeed strongly enhanced by NT practices in which SOM plays a crucial role (Baldock and Skjemstad, 2000; Balesdent et al., 2000; Chenu et al., 2019; Lal, 2004; Oades, 1984; Paustian et al., 1997; Six et al., 1999; Six et al., 2000a,b; Six et al., 2004; Six and Paustian, 2014; Stockmann et al., 2013; Wiesmeier et al., 2019). The contribution of free microaggregates to the phytolith pool reaches nearly 75% in NT and 63% in CT (Fig. 7a), whereas their

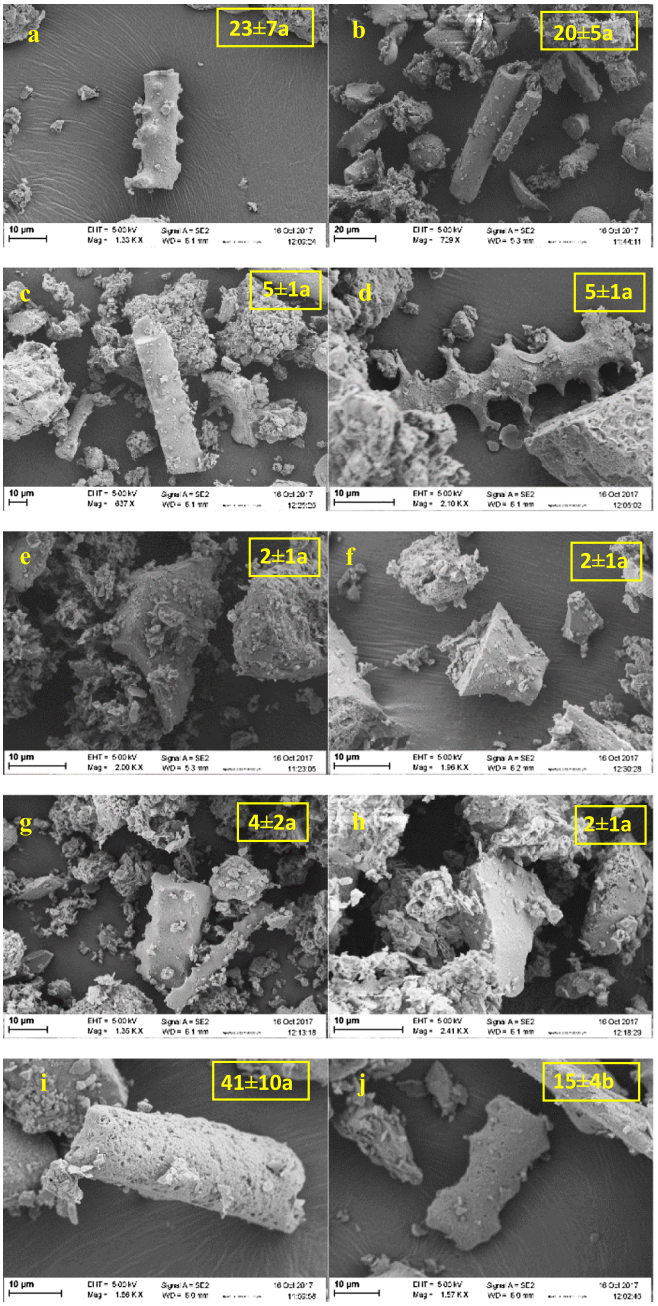

Fig. 6. SEM images of phytoliths isolated from bulk soil and aggregate fractions in CT (left: a-i) and NT (right: b-j). Phytoliths extracted from (a) and (b): bulk soil; (c) and (d): macroaggregates; (e) and (f): free microaggregates; (g) and (h): protected microaggregates; (i) and (j): silt + clay. Number indicates a precise counting of the dissolution cavities (per 100 μm^2) performed on the microphotographs. The average values shown with distinct letters (a, b) between CT and NT are significantly different at the $p < 0.01$ confidence level according to independent-Samples T– separation test ($n > 3$).

contribution to the pool of bioavailable Si reaches 62% in NT and 53% in CT (Fig. 7c). These findings highlight that free microaggregates contribute majorly to the pools of soil phytoliths and bioavailable Si (Fig. 7). Thus, NT practices enhance the formation of microaggregates (Fig. 2), which store phytoliths and hence bioavailable Si. Indeed, as compared to CT, NT exhibits a smaller proportion of macroaggregates, protected microaggregates and silt + clay, while it has a greater proportion of free microaggregates (Fig. 2). This experimental fact corroborates previous studies (Six et al., 1999; Six et al., 2000b), showing that, relatively to CT, the turnover rate of macroaggregate formation

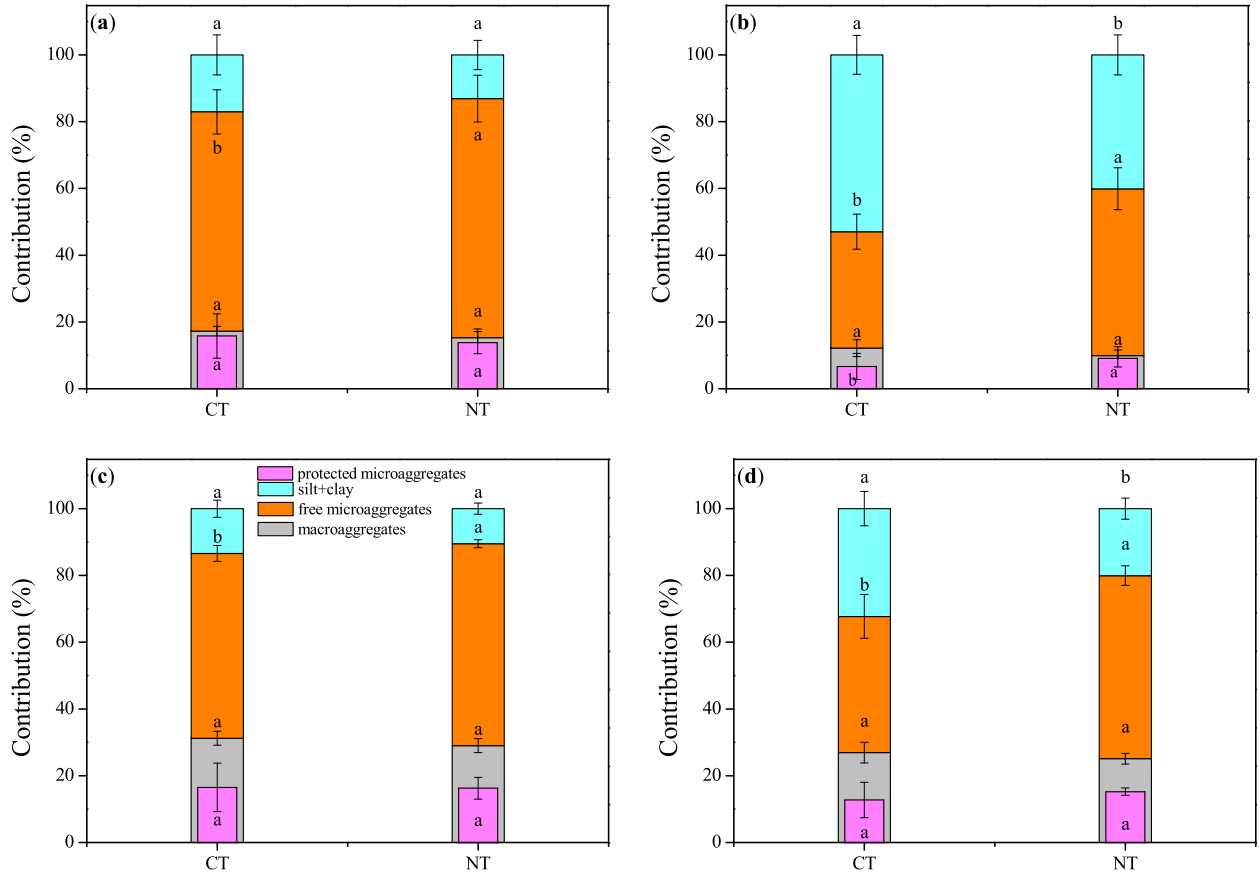

Fig. 7. Stacker bars plots of the respective contributions to bulk soil of the extracted Si (a-c) and total carbon (d) stocks within aggregates: (a) *hl*PhSi, (b) Na_2CO_3-Si, (c) $CaCl_2$-Si, (d) total C contents under CT and NT. Different lowercase letter (a, b) resulting from the *independent samples T – separation test* are given for comparisons between CT and NT (n = 9, $p < 0.05$).

and degradation is slower under NT, hence yielding less protected microaggregates and silt + clay, but more free microaggregates (Six et al., 2000a). Microaggregates rather than macroaggregates protect SOM in the long term whereas macroaggregate turnover is a crucial process influencing the stabilization of SOM (Six et al., 2000a,b). The rate of macroaggregate turnover is reduced under NT compared to CT, which leads to the formation of stable microaggregates in which carbon may be stabilized and protected in the long term (Six et al., 2002). In contrast, in CT, the periodical perturbation of soil aggregates by tillage practices increases SOM decomposition rates by exposing SOM that is physically protected in soil aggregates (Balesdent et al., 2000; Six et al., 2002). The increase in phytolith stocks in free and protected microaggregates reveals the retention of phytoliths in microaggregates, and this retention is larger in NT than in CT (Figs. 4a and 8a). Thus, the larger phytolith pool (*hl*PhSi) in microaggregates improves the reservoir of $CaCl_2$-Si in protected and free microaggregates in NT relatively to CT (Figs. 4a and 8a). CT practices involving repeated and intensive tillage enhance the turnover of macroaggregates (Bronick and Lal, 2005; Six et al., 1999). In contrast, a slow turnover in NT stabilizes SOM in soil aggregates (Six et al., 2002; Six et al., 1999; Six and Paustian, 2014; Fig. 8d). It likely protects phytoliths from rapid dissolution under the physical protection similarly to SOC, hence increasing the pool of bioavailable Si (Figs. 4, 7, 8), as illustrated by the much lower density of phytolith dissolution cavities in soil aggregates as compared to the silt + clay fraction (Fig. 6). The physical protection likely decreases the dissolution rate of phytoliths probably because of a gradient of H_4SiO_4 concentration in the soil solution that encompasses a liquid phase held in pores of varying sizes and thus at different hydric potentials (Gérard et al., 2008). However, this remains speculative. Stored SOM may indirectly affect phytoliths since SOM is involved in aggregation.

Therefore, phytoliths held within microaggregates are major contributors to the pool of bioavailable Si as illustrated in Fig. 8. This graph further shows that for a given soil phytolith content, $CaCl_2$-Si content of most macro- and microaggregates is larger than the one in silt + clay. Phytoliths in silt + clay fractions in either CT or NT are likely more weathered (Fig. 6i-j) than in other soil aggregate fractions (Fig. 6c–h). Weathered phytoliths may be less soluble than fresh ones, notably because a decrease of surface area with increasing age (Meunier et al., 2014; Puppe and Leue, 2018). In this regard, possible mechanisms encompass the presence of organic matter bound to phytoliths (Bartoli, 1985; Fraysse et al., 2009) and/or the Al coating of phytolith surface (Bartoli, 1985; Bartoli and Wilding, 1980). Fig. 5 supports the hypothesis of a lesser release of $CaCl_2$-Si from phytoliths in silt + clay, since the extraction rate of Si in $CaCl_2$ rapidly decreased in silt + clay fraction (Fig. 5e). However, in the macro and microaggregates (Fig. 5b–d), the extraction kinetics did not reach a plateau, particularly in free microaggregates, as previously observed on pure phytoliths (Georgiadis et al., 2013).

4.4. The DeMaster technique likely underestimates the pool of phytoliths in the studied soil

Alkaline extraction is known to extract not only biogenic silica, but also non-biogenic or pedogenic amorphous Si forms (e.g., Saccone et al., 2007; Georgiadis et al., 2013, 2014). The corresponding correction method according to DeMaster (1981) was questioned recently (Meunier et al., 2014; Li et al., 2019, Kaczorek et al., 2019) since Na_2CO_3 does not selectively dissolve phytoliths. Our data corroborate these studies. Small water-soluble phytogenic particles (< 5μm) (Puppe

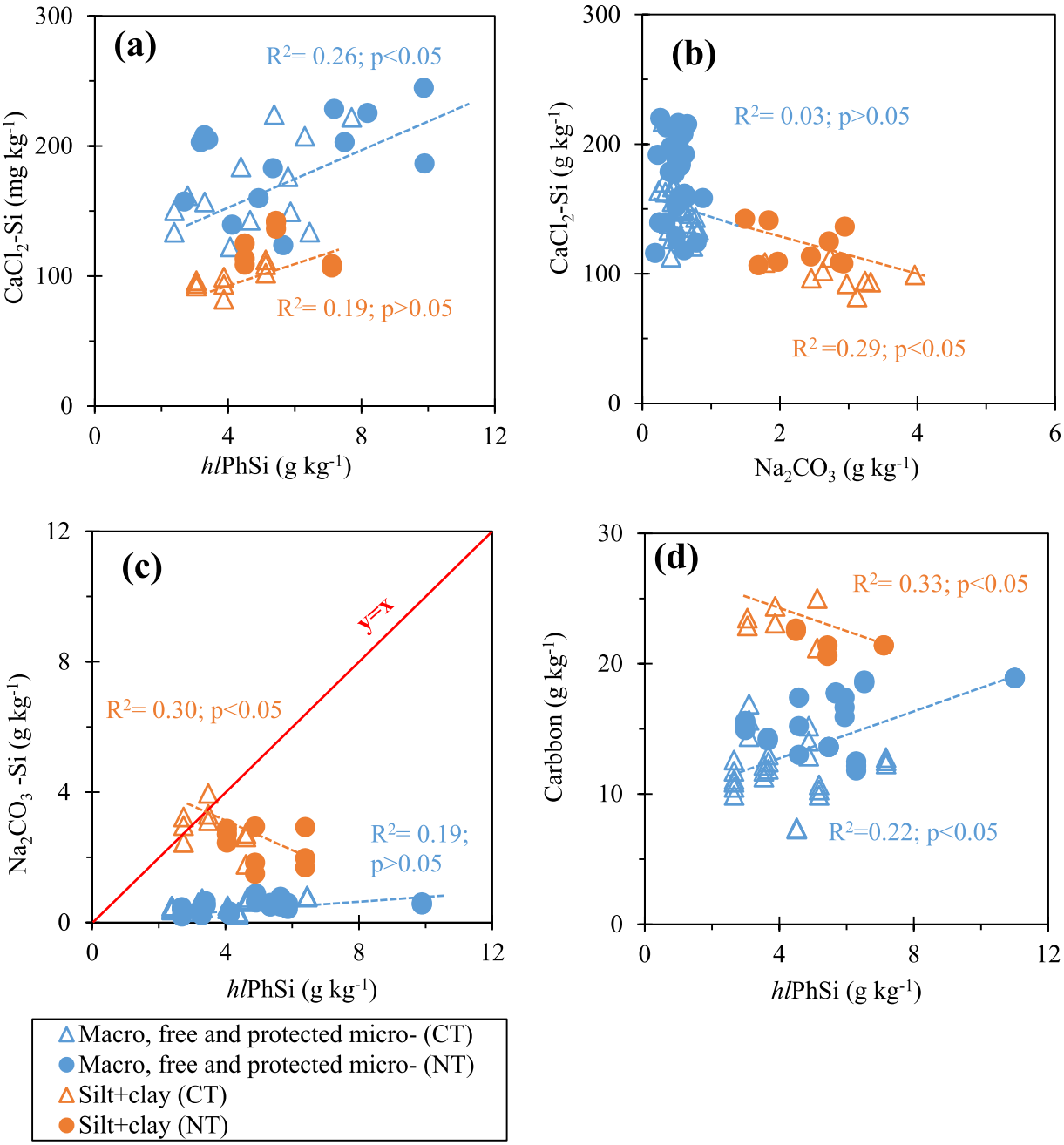

Fig. 8. Relationships between $CaCl_2$-Si concentration and (a) *hl*PhSi content, (b) Na_2CO_3-Si concentration, (c) between Na_2CO_3-Si concentration and *hl*PhSi content; and (d) between carbon content and *hl*PhSi content (d).

et al., 2017), which can dissolve in Na_2CO_3, would be excluded after physical extraction if they are smaller than 2 μm due to the filtration step. Here, Fig. 8c shows that Na_2CO_3-Si is smaller than *hl*PhSi physically extracted by heavy liquid separation, except for some silt + clay samples in CT where Na_2CO_3-Si and *hl*PhSi contents are similar. Besides, $CaCl_2$-Si and Na_2CO_3-Si are not correlated to each other (Fig. 8b). In addition to these experimental facts, Na_2CO_3-Si is much larger in silt + clay than in bulk soil and soil aggregates (Fig. 4c). Probably, silicate minerals in silt + clay may be more soluble at pH 11 (Na_2CO_3) than in aggregate fractions. In field conditions, phytoliths entrapped in soil microaggregates likely dissolve very little and might remain fresh whereas free phytoliths present in silt + clay could be more weathered (Fig. 6i-j). Based on this, the dissolution of free phytoliths in silt + clay rapidly reaches a steady state. The very poor correlation between Na_2CO_3-Si and *hl*PhSi (Fig. 8c), particularly in soil aggregates, supports the assumption that Na_2CO_3 preferentially dissolves free phytoliths (Fig. 8c) and relatively fresh ones (Meunier et al., 2014). Both entrapped and fresh phytoliths in microaggregates release Si in $CaCl_2$ (Fig. 8a) whereas both free and weathered phytoliths in silt + clay release little Si (Fig. 8a). We can conclude as follows: (i) Na_2CO_3 quantifies fresh and free phytoliths; (ii) phytoliths entrapped in microaggregates are protected in soils, but not in the $CaCl_2$ solution in which they release Si. During the $CaCl_2$ extraction, the solid-liquid shaking may promote abrasion (McKeague and Cline, 1963; Schachtschabel and Heinemann, 1967) and, therefore the release of fresh phytoliths previously entrapped in the microaggregates.

5. Conclusion

In the studied sandy loam, (i) Na_2CO_3 quantifies fresh and free

phytoliths; (ii) phytoliths entrapped in microaggregates are protected in soils, but not in the $CaCl_2$ solution in which they slowly release Si; (iii) soil microaggregates contribute for more than 75% to the phytolith pool and that of bioavailable Si; (iv) phytolith dissolution features are virtually absent in soil aggregates. Consequently, the release of bioavailable Si from microaggregates is slower than that from the silt + clay fraction. No-tillage practices and associated agricultural techniques, may thus promote the preservation of phytoliths in soils and their slow release as they stabilize SOM in the long term. Soil microaggregates can therefore protect phytoliths from dissolution, just as they protect SOM from biodegradation. We believe that the entrapment of phytoliths in soil aggregates may be one of the processes favoring the persistence of phytoliths in soils and sediments. We expect that this persistence may be enhanced in strongly aggregated soils, such as Chernozems. This finding opens new routes to understand the fate of Si in the soil-to-plant cycle. We also hypothesize that small phytogenic particles (< 5 μm), an important and reactive reservoir of Si in soils (Puppe et al. 2017), could interact primarily with soil colloids in the aggregation process. Furthermore, future research should aim to understand an apparent paradox. On one hand, phytoliths are considered by scientists in the field of biogeochemistry as the major pool of mobile Si in the soil-to-plant system because of their high dissolution rate. On the other hand, they are used in other disciplines as microfossils to reconstruct paleoenvironments because of their stability over millennia (Cabanes and Shahack-Gross, 2015; Piperno, 2006; Piperno and Pearsall, 1998; Strömberg et al., 2018). Evidently, we expect that soil properties and processes impact or govern both of these pathways in a given environmental framework. This emerging vision opens new routes to study the biogeochemical cycle of silicon.

Acknowledgements

We thank A. Iserentant and C. Givron for laboratory assistance and technical advice (UCLouvain). We express our gratitude to Prof. Ch. Bielders for his pertinent comments and advices. We sincerely thank the three anonymous reviewers and the Associate Editor for their pertinent advices and sound recommendations. Z. Li is supported by the 'Fonds Spécial de Recherche' (FSR) of the UClouvain (fsr-2014), the Aspirant (ASP) – 'Fonds National de la Recherche Scientifique' (FNRS) and Chargé de recherches (CR) – FNRS of Belgium. F. de Tombeur is supported by the Crédit de recherche (CDR)-FNRS. All authors contributed to paper writing and revision. The authors declare that there are no conflicts of interest.

Appendix A. Supplementary data

Supplementary data to this article can be found online at https://doi.org/10.1016/j.geoderma.2019.114037.

References

Abiven, S., Menasseri, S., Chenu, C., 2009. The effects of organic inputs over time on soil aggregate stability–a literature analysis. Soil Biol. Biochem. 41 (1), 1–12.
Alexandre, A., Meunier, J.-D., Colin, F., Koud, J.-M., 1997. Plant impact on the biogeochemical cycle of silicon and related weathering processes. Geochim. Cosmochim. Acta 61 (3), 677–682.
Baldock, J., Skjemstad, J., 2000. Role of the soil matrix and minerals in protecting natural organic materials against biological attack. Org. Geochem. 31 (7–8), 697–710.
Balesdent, J., Chenu, C., Balabane, M., 2000. Relationship of soil organic matter dynamics to physical protection and tillage. Soil Tillage Res. 53 (3–4), 215–230.
Bartoli, F., 1983. The biogeochemical cycle of silicon in two temperate forest ecosystems. Ecol. Bull. 469–476.
Bartoli, F., 1985. Crystallochemistry and surface properties of biogenic opal. Eur. J. Soil Sci. 36 (3), 335–350.
Bartoli, F., Wilding, L., 1980. Dissolution of biogenic opal as a function of its physical and chemical properties. Soil Sci. Soc. Am. J. 44 (4), 873–878.
Berner, R.A., 1997. The rise of plants and their effect on weathering and atmospheric CO2. Science 276 (5312), 544–546.
Blanco-Canqui, H., Lal, R., 2008. No-tillage and soil-profile carbon sequestration: an on-farm assessment. Soil Sci. Soc. Am. J. 72 (3), 693–701.
Blecker, S.W., McCulley, R.L., Chadwick, O.A., Kelly, E.F., 2006. Biologic cycling of silica across a grassland bioclimosequence. Global Biogeochem. Cycles 20 (3).
Bronick, C.J., Lal, R., 2005. Soil structure and management: a review. Geoderma 124 (1–2), 3–22.
Cabanes, D., Shahack-Gross, R., 2015. Understanding fossil phytolith preservation: the role of partial dissolution in paleoecology and archaeology. PLoS One 10 (5), e0125532.
Carey, J.C., Fulweiler, R.W., 2016. Human appropriation of biogenic silicon–the increasing role of agriculture. Funct. Ecol. 30 (8), 1331–1339.
Chao, T., Sanzolone, R., 1992. Decomposition techniques. J. Geochem. Explor. 44 (1–3), 65–106.
Chapman, H., 1965. Cation-exchange capacity. Methods of soil analysis. Part 2. Chemical and microbiological properties (methodsofsoilanb), 891–901.
Chenu, C., Angers, D.A., Barré, P., Derrien, D., Arrouays, D., Balesdent, J., 2019. Increasing organic stocks in agricultural soils: knowledge gaps and potential innovations. Soil Tillage Res. 188, 41–52.
Clymans, W., Struyf, E., Govers, G., Vandevenne, F., Conley, D., 2011. Anthropogenic impact on amorphous silica pools in temperate soils. Biogeosciences 8 (8), 2281–2293.
Conley, D.J., 2002. Terrestrial ecosystems and the global biogeochemical silica cycle. Global Biogeochem. Cycles 16 (4).
Cornelis, J.-T., Delvaux, B., Cardinal, D., André, L., Ranger, J., Opfergelt, S., 2010. Tracing mechanisms controlling the release of dissolved silicon in forest soil solutions using Si isotopes and Ge/Si ratios. Geochim. Cosmochim. Acta 74 (14), 3913–3924.
Cornelis, J.-T., Titeux, H., Ranger, J., Delvaux, B., 2011. Identification and distribution of the readily soluble silicon pool in a temperate forest soil below three distinct tree species. Plant Soil 342 (1–2), 369–378.
Coskun, D., Deshmukh, R., Sonah, H., Menzies, J.G., Reynolds, O., Ma, J.F., Kronzucker, H.J., Bélanger, R.R., 2019. The controversies of silicon's role in plant biology. New Phytol. 221 (1), 67–85.
Cornelis, J.T., Delvaux, B., 2016. Soil processes drive the biological silicon feedback loop. Funct. Ecol. 30 (8), 1298–1310.
De Tombeur, F., Sohy, V., Chenu, C., Colinet, G., Cornelis, J.-T., 2018. Effects of permaculture practices on soil physico-chemical properties and organic matter distribution in aggregates: a case study of the Bec-Hellouin farm (France). Front. Environ. Sci. 6, 116.
DeMaster, D.J., 1981. The supply and accumulation of silica in the marine environment. Geochim. Cosmochim. Acta 45 (10), 1715–1732.
Desplanques, V., Cary, L., Mouret, J.-C., Trolard, F., Bourrié, G., Grauby, O., Meunier, J.-D., 2006. Silicon transfers in a rice field in Camargue (France). J. Geochem. Explor. 88 (1–3), 190–193.
Fraysse, F., Pokrovsky, O.S., Schott, J., Meunier, J.-D., 2009. Surface chemistry and reactivity of plant phytoliths in aqueous solutions. Chem. Geol. 258 (3), 197–206.
Fraysse, F., Pokrovsky, O.S., Schott, J., Meunier, J., 2006. Surface properties, solubility and dissolution kinetics of bamboo phytoliths. Geochim. Cosmochim. Acta 70 (8), 1939–1951.
Georgiadis, A., Sauer, D., Herrmann, L., Breuer, J., Zarei, M., Stahr, K., 2013. Development of a method for sequential Si extraction from soils. Geoderma 209, 251–261.
Georgiadis, A., Sauer, D., Herrmann, L., Breuer, J., Zarei, M., Stahr, K., 2014. Testing a new method for sequential silicon extraction on soils of a temperate–humid climate. Soil Res. 52 (7), 645–657.
Gérard, F., Mayer, K., Hodson, M., Ranger, J., 2008. Modelling the biogeochemical cycle of silicon in soils: application to a temperate forest ecosystem. Geochim. Cosmochim. Acta 72 (3), 741–758.
Guntzer, F., Keller, C., Poulton, P.R., McGrath, S.P., Meunier, J.-D., 2012. Long-term removal of wheat straw decreases soil amorphous silica at Broadbalk. Rothamsted. Plant and Soil 352 (1–2), 173–184.
Haynes, R.J., 2017. The nature of biogenic Si and its potential role in Si supply in agricultural soils. Agric. Ecosyst. Environ. 245, 100–111.
Haysom, M., Chapman, L., 1975. Some aspects of the calcium silicate trials at Mackay, Proceedings.
Henriet, C., De Jaeger, N., Dorel, M., Opfergelt, S., Delvaux, B., 2008. The reserve of weatherable primary silicates impacts the accumulation of biogenic silicon in volcanic ash soils. Biogeochemistry 90 (2), 209–223.
Herbillon, A., 1986. Chemical estimation of weatherable minerals present in the diagnostic horizons of low activity clay soils, Proceedings of the 8th International Clay Classification Workshop: Classification, Characterization and Utilization of Oxisols (part 1)[Beinroth, FH, Camargo, MN and Eswaran (ed.)][39–48](Rio de Janeiro, 1986).
IUSS, 2014. World Reference Base for Soil Resources 2014 International Soil Classification System for Naming Soils and Creating Legends for Soil Maps. FAO, Rome.
Kaczorek, D., Puppe, D., Busse, J., Sommer, M., 2019. Effects of phytolith distribution and characteristics on extractable silicon fractions in soils under different vegetation–an exploratory study on loess. Geoderma 356, 113917.
Karathanasis, A., 2002. Mineral equilibria in environmental soil systems. Soil Mineral. Environ. Appl. 109–151.
Keller, C., Guntzer, F., Barboni, D., Labreuche, J., Meunier, J.-D., 2012. Impact of agriculture on the Si biogeochemical cycle: input from phytolith studies. C.R. Geosci. 344 (11), 739–746.
Kelly, E., 1990. Methods for extracting opal phytoliths from soil and plant material, Workshop on biotic indicators of global change, University of Washington (Seattle).
Kleber, M., Eusterhues, K., Keiluweit, M., Mikutta, C., Mikutta, R., Nico, P.S., 2015. Mineral–organic associations: formation, properties, and relevance in soil environments. In: Advances in Agronomy. Elsevier, pp. 1–140.

Klotzbücher, T., Marxen, A., Vetterlein, D., Schneiker, J., Türke, M., van Sinh, N., Manh, N.H., van Chien, H., Marquez, L., Villareal, S., 2015. Plant-available silicon in paddy soils as a key factor for sustainable rice production in Southeast Asia. Basic Appl. Ecol. 16 (8), 665–673.
Koning, E., Epping, E., Van Raaphorst, W., 2002. Determining biogenic silica in marine samples by tracking silicate and aluminium concentrations in alkaline leaching solutions. Aquat. Geochem. 8 (1), 37–67.
Lal, R., 2004. Soil carbon sequestration impacts on global climate change and food security. Science 304(5677), 1623–1627.
Li, Z., Song, Z., Cornelis, J.-T., 2014. Impact of rice cultivar and organ on elemental composition of phytoliths and the release of bio-available silicon. Frontiers in Plant Sci. 5.
Li, Z., Unzué-Belmonte, D., Cornelis, J.-T., Linden, C.V., Struyf, E., Ronsse, F., Delvaux, B., 2019. Effects of phytolithic rice-straw biochar, soil buffering capacity and pH on silicon bioavailability. Plant Soil 438 (1–2), 187–203.
Lindsay, W.L., 1979. Chemical Equilibria in Soils. John Wiley and Sons Ltd.
Lucas, Y., Luizao, F., Chauvel, A., Rouiller, J., Nahon, D., 1993. The relation between biological activity of the rain forest and mineral composition of soils. Science 260 (5107), 521–523.
Makabe, S., KAKUDA, K.i., Sasaki, Y., Ando, T., Fujii, H., Ando, H., 2009. Relationship between mineral composition or soil texture and available silicon in alluvial paddy soils on the Shounai Plain, Japan. Soil Sci. Plant Nutrit. 55(2), 300–308.
Matichenkov, V., Bocharnikova, E., 2001. The relationship between silicon and soil physical and chemical properties. In: Studies in Plant Science. Elsevier, pp. 209–219.
McKeague, J., Cline, M., 1963. Silica in soil solutions: II. The adsorption of monosilicic acid by soil and by other substances. Can. J. Soil Sci. 43 (1), 83–96.
Melzer, S.E., Chadwick, O.A., Hartshorn, A.S., Khomo, L.M., Knapp, A.K., Kelly, E.F., 2012. Lithologic controls on biogenic silica cycling in South African savanna ecosystems. Biogeochemistry 108 (1–3), 317–334.
Meunier, J.-D., Sandhya, K., Prakash, N.B., Borschneck, D., Dussouillez, P., 2018. pH as a proxy for estimating plant-available Si? a case study in rice fields in Karnataka (South India). Plant Soil 432 (1–2), 143–155.
Meunier, J.D., Keller, C., Guntzer, F., Riotte, J., Braun, J.J., Anupama, K., 2014. Assessment of the 1% Na2CO3 technique to quantify the phytolith pool. Geoderma 216, 30–35.
Meyer, J., Keeping, M., 2001. Past, present and future research of the role of silicon for sugarcane in southern Africa. Plant Sci. J. 8, 257–275.
Oades, J.M., 1984. Soil organic matter and structural stability: mechanisms and implications for management. Plant Soil 76 (1–3), 319–337.
Paustian, K., Collins, H.P., Paul, E.A., 1997. Management Controls on Soil Carbon. CRC Press, Boca Raton, FL, USA.
Piperno, D.R., 2006. Phytoliths: A Comprehensive Guide for Archaeologists and Paleoecologists. Rowman Altamira.
Piperno, D.R., Pearsall, D.M., 1998. The silica bodies of tropical American grasses: morphology, taxonomy, and implications for grass systematics and fossil phytolith identification. Smithsonian contributions to botany.
Poeplau, C., Don, A., 2015. Carbon sequestration in agricultural soils via cultivation of cover crops–a meta-analysis. Agric. Ecosyst. Environ. 200, 33–41.
Puppe, D., Ehrmann, O., Kaczorek, D., Wanner, M., Sommer, M., 2015. The protozoic Si pool in temperate forest ecosystems—quantification, abiotic controls and interactions with earthworms. Geoderma 243, 196–204.
Puppe, D., Höhn, A., Kaczorek, D., Wanner, M., Wehrhan, M., Sommer, M., 2017. How big is the influence of biogenic silicon pools on short-term changes in water-soluble silicon in soils? Implications from a study of a 10-year-old soil–plant system. Biogeosciences 14, 5239–5252.
Puppe, D., Leue, M., 2018. Physicochemical surface properties of different biogenic silicon structures: results from spectroscopic and microscopic analyses of protistic and phytogenic silica. Geoderma 330, 212–220.
Rouiller, J., Burtin, G., Souchier, B., 1972. dispersion des sols dans l'analyse granulometrique, methode utilisant les resines echangeuses d'ions. Nancy Ecole Nat Super Agron Bull.
Saccone, L., Conley, D., Koning, E., Sauer, D., Sommer, M., Kaczorek, D., Blecker, S., Kelly, E., 2007. Assessing the extraction and quantification of amorphous silica in soils of forest and grassland ecosystems. Eur. J. Soil Sci. 58 (6), 1446–1459.
Saccone, L., Conley, D., Sauer, D., 2006. Methodologies for amorphous silica analysis. J. Geochem. Explor. 88 (1–3), 235–238.
Sauer, D., Saccone, L., Conley, D.J., Herrmann, L., Sommer, M., 2006. Review of methodologies for extracting plant-available and amorphous Si from soils and aquatic sediments. Biogeochemistry 80 (1), 89–108.
Schachtschabel, P., Heinemann, C., 1967. Wasserlösliche kieselsäure in lößböden. Zeit. Pflanzenernährung Bodenkunde 118 (1), 22–35.
Six, J., Conant, R., Paul, E.A., Paustian, K., 2002. Stabilization mechanisms of soil organic matter: implications for C-saturation of soils. Plant Soil 241 (2), 155–176.
Six, J., Elliott, E., Paustian, K., 1999. Aggregate and soil organic matter dynamics under conventional and no-tillage systems. Soil Sci. Soc. Am. J. 63 (5), 1350–1358.
Six, J., Elliott, E., Paustian, K., Doran, J., 1998. Aggregation and soil organic matter accumulation in cultivated and native grassland soils. Soil Sci. Soc. Am. J. 62 (5), 1367–1377.
Six, J., Elliott, E.T., Paustian, K., 2000a. Soil macroaggregate turnover and microaggregate formation: a mechanism for C sequestration under no-tillage agriculture. Soil Biol. Biochem. 32 (14), 2099–2103.
Six, J., Ogle, S.M., Conant, R.T., Mosier, A.R., Paustian, K., 2004. The potential to mitigate global warming with no-tillage management is only realized when practised in the long term. Glob. Change Biol. 10 (2), 155–160.
Six, J., Paustian, K., Elliott, E.T., Combrink, C., 2000b. Soil structure and organic matter I. Distribution of aggregate-size classes and aggregate-associated carbon. Soil Sci. Soc. Am. J. 64 (2), 681–689.
Six, J., Paustian, K., 2014. Aggregate-associated soil organic matter as an ecosystem property and a measurement tool. Soil Biol. Biochem. 68, A4–A9.
Smithson, F., 1956. Plant opal in soil. Nature 178 (4524), 107.
Stockmann, U., Adams, M.A., Crawford, J.W., Field, D.J., Henakaarchchi, N., Jenkins, M., Minasny, B., McBratney, A.B., De Courcelles, V.d.R., Singh, K., 2013. The knowns, known unknowns and unknowns of sequestration of soil organic carbon. Agriculture, Ecosystems Environment 164, 80–99.
Strömberg, C.A., Dunn, R.E., Crifò, C., Harris, E.B., 2018. Phytoliths in paleoecology: analytical considerations, current use, and future directions. In: Methods in Paleoecology. Springer, pp. 235–287.
Struyf, E., Smis, A., Van Damme, S., Garnier, J., Govers, G., Van Wesemael, B., Conley, D.J., Batelaan, O., Frot, E., Clymans, W., 2010. Historical land use change has lowered terrestrial silica mobilization. Nat. Commun. 1, 129.
Totsche, K.U., Amelung, W., Gerzabek, M.H., Guggenberger, G., Klumpp, E., Knief, C., Lehndorff, E., Mikutta, R., Peth, S., Prechtel, A., 2018. Microaggregates in soils. J. Plant Nutr. Soil Sci. 181 (1), 104–136.
Vandevenne, F., Barão, L., Ronchi, B., Govers, G., Meire, P., Kelly, E., Struyf, E., 2015. Silicon pools in human impacted soils of temperate zones. Global Biogeochem. Cycles 29 (9), 1439–1450.
Vandevenne, F., Struyf, E., Clymans, W., Meire, P., 2012. Agricultural silica harvest: have humans created a new loop in the global silica cycle? Front. Ecol. Environ. 10 (5), 243–248.
West, T.O., Post, W.M., 2002. Soil organic carbon sequestration rates by tillage and crop rotation. Soil Sci. Soc. Am. J. 66 (6), 1930–1946.
White, A.F., Vivit, D.V., Schulz, M.S., Bullen, T.D., Evett, R.R., Aagarwal, J., 2012. Biogenic and pedogenic controls on Si distributions and cycling in grasslands of the Santa Cruz soil chronosequence, California. Geochim. Cosmochim. Acta 94, 72–94.
Wiesmeier, M., Urbanski, L., Hobley, E., Lang, B., von Lützow, M., Marin-Spiotta, E., van Wesemael, B., Rabot, E., Ließ, M., Garcia-Franco, N., 2019. Soil organic carbon storage as a key function of soils-A review of drivers and indicators at various scales. Geoderma 333, 149–162.